Antagonism between fine and coarse motion sensors depends on stimulus size and contrast

Ignacio Serrano-Pedraza

Institute of Neuroscience, Newcastle University, Newcastle upon Tyne, UK

Andrew M. Derrington

School of Psychology, University of Liverpool, Liverpool, UK

The perceived direction of motion of a brief visual stimulus that contains fine features reverses if static coarser features are added to it. Here we show that the reversal in perceived direction disappears if the stimulus is reduced in size from 2.8 deg to 0.35 deg radius. We show that for a stimulus with 1.4 deg radius, the reversals occur when the ratio between the contrast of the fine features and of the coarser features is higher than 0.8 and lower than 4. For stimulus with 0.35 deg radius, the reversals never appear for any contrast ratio. We also show that if the stimulus is presented within an annular window with small radius, errors disappear but they return if the radius is increased to 2 deg. The errors in motion discrimination described here can be explained by a model of motion sensing in which the signals from fine-scale and coarse-scale sensors are subtracted from one another (I. Serrano-Pedraza, P. Goddard, & A. M. Derrington, 2007). The model produces errors in direction when the signals in the fine and coarse sensors are approximately balanced. The errors disappear when stimulus size is reduced because the reduction in size differentially reduces the response of the low spatial frequency motion sensors.

Keywords: motion, temporal vision, motion energy detector, motion impairments, inhibition, interaction between motion sensors

Citation: Serrano-Pedraza, I., & Derrington, A. M. (2010). Antagonism between fine and coarse motion sensors depends on stimulus size and contrast. *Journal of Vision, 10*(8):18, 1–12, http://www.journalofvision.org/content/10/8/18, doi:10.1167/10.8.18.

Introduction

In a moving natural image, there are physical features with different spatial scales that can be analyzed by the human visual system. There is considerable data consistent with the idea that early processing by the human visual system analyzes fine-scale and coarse-scale image features separately. For example, the idea that motion sensors in the human visual system are selective for spatial frequency and have localized receptive fields has been supported by experiments using spatial summation and masking (Anderson & Burr, 1985; Anderson & Burr, 1987; Anderson & Burr, 1989; Anderson & Burr, 1991; Anderson, Burr, & Morrone, 1991). Models of human visual motion sensing also have long assumed that the basic motion sensor is selective for spatial frequency, orientation, and location (Adelson & Bergen, 1985; Watson & Ahumada, 1985). Given that motion signals from different spatial scales are analyzed by different sets of motion sensors, it is theoretically possible to combine the outputs of the motion sensors in ways that facilitate some visual tasks at the expense of others.

We have shown previously that motion discrimination is a task in which performance suffers when the stimulus contains features designed to activate both fine-scale and coarse-scale sensors. When human observers are required to discriminate the direction of motion of very brief stimuli, they make systematic errors when the moving stimuli contain features that have two different spatial scales (Derrington, Fine, & Henning, 1993; Derrington & Henning, 1987; Henning & Derrington, 1988; Serrano-Pedraza & Derrington, 2008; Serrano-Pedraza, Goddard, & Derrington, 2007). In particular, the perceived direction of motion of a complex stimulus that consists of a moving fine-scale (high spatial frequency) pattern added to a static coarse-scale (low spatial frequency) pattern is completely reversed at short durations. Similar systematic errors occur with a variety of different types of spatial patterns that include moving fine-scale and static coarse-scale features, including gratings, anisotropic noise, and isotropic noise. The errors can be reproduced by a model of motion sensing in which there is a subtractive interaction between motion sensors tuned to high spatial frequencies and those tuned to low spatial frequencies (Serrano-Pedraza et al., 2007).

In this paper, we extend our studies of the systematic errors in perceived direction of motion that occur when the stimulus contains both coarse-scale and fine-scale features. Our aim is to characterize the conditions under which motion sensing is impaired in order to identify what may be the tasks in which performance could potentially

doi: 10.1167/10.8.18 Received February 24, 2010; published July 23, 2010 ISSN 1534-7362

be enhanced. In this paper, we explore the effect of varying the dimensions of circular and annular stimuli and of varying the contrast of the stimulus components.

In most previous experiments, the complex stimuli covered a large area of the retina. They either had no spatial windows (Derrington & Henning, 1987; Henning & Derrington, 1988) or large, two-dimensional Gaussian windows (Serrano-Pedraza et al., 2007). Consequently our first aim is to explore the importance of stimulus size examining whether similar errors occur when the size of the stimulus is systematically reduced by using progressively smaller Gaussian windows. We found that the errors are no longer apparent when the stimulus size is reduced.

Our second aim is to explore effects of contrast. Previous experiments demonstrated that reversed apparent motion only occurs when the ratio between the contrast of fine and coarser features is situated within a certain range. This suggests that the motion signals in high spatial frequency-selective and low spatial frequency-selective mechanisms must be balanced against each other (Derrington & Henning, 1987).

With these two aims, we did three experiments. First, we measured the discrimination of motion direction of simple and complex moving stimuli (anisotropic noise containing fine-scale and coarse-scale features) that were windowed by Gaussian windows of different sizes centered on the fovea. In the second experiment, we used similar anisotropic noise with annular spatial windows with different eccentricities in order to present the stimuli in the near retinal periphery.

These first two experiments revealed that reversals in motion direction occur only with large windows, either Gaussian or annular. In the third experiment, we investigate

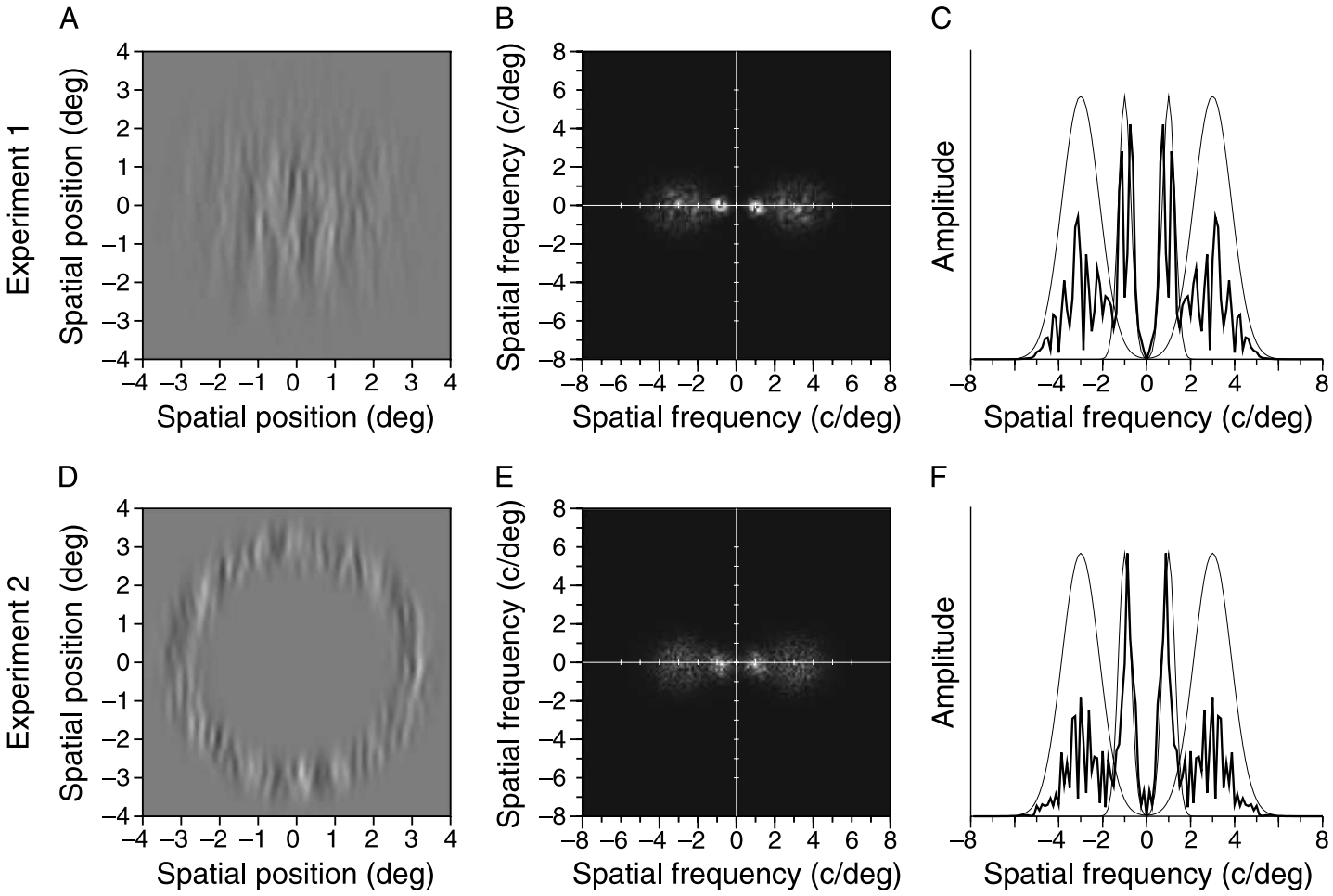

Figure 1. Examples of the stimuli used in Experiments 1 and 2. The complex stimuli are constructed by adding two anisotropic filtered noise samples with filter center frequencies of 1 and 3 cycles/deg. The root-mean-squared contrast of each filtered noise was 0.0748. (a) Example of complex stimulus with Gaussian window (Experiment 1) with σ_{xy} = 1.4 deg. (b) Two-dimensional Fourier amplitude spectrum of (a). (c) Thick line: amplitude spectrum profile of (b); thin line: profile of the filters (see Equation 3) used to construct the anisotropic noise samples. (d) Example of complex stimulus with annular window (Experiment 2) with radius r_i = 3 deg and σ_{xy} = 0.35 deg. (e) Two-dimensional Fourier amplitude spectrum of (d). (f) Thick line: amplitude spectrum profile of (e); thin line: profile of the filters (see Equation 3) used to construct the anisotropic noise.

the range of contrast ratios at which reversals in perceived direction of motion occur, using windows of two different sizes, one very small (σ_{xy} = 0.35 deg) and other large (σ_{xy} = 1.4 deg). For very small stimuli, the reversals did not appear for any contrast ratio.

Finally, using the same stimuli and conditions used in the experiments, we performed simulations using the model developed by Serrano-Pedraza et al. (2007). The model reproduces the errors in perceived direction of motion and the way that they depend on the characteristics of the spatial windows, exactly as observed in the psychophysical experiments.

Methods

Subjects

Four human subjects, two males (IS and AD, the authors) and two females (ER and RL) took part in Experiments 1 and 2; and two subjects (IS and AD) in Experiment 3. The subjects ER and RL were not aware of the purpose of the study. All subjects had normal or corrected-to-normal refraction and normal visual acuity. The experiments were carried out in a dark room and a chin rest (UHCOTech HeadSpot) was used to stabilize the subject's head and to control the observation distance. Subjects viewed the screen binocularly with natural pupils. To minimize tracking eye movements, the subjects were instructed to maintain fixation on a small cross (0.25° × 0.25°) in the center of the screen before presenting the stimuli. Experimental procedures were approved by the Psychology Ethics Committee of Newcastle University.

Stimulus presentation

In Experiments 1 and 2, stimuli were presented on a gamma-corrected 22″ monitor (Mitsubishi Diamond pro 2020U) under the control of an Apple Macintosh G5. In Experiment 3, a 19″ ViewSonic G90fB monitor was used under the control of an Apple Macintosh Pro using Bits++ (Cambridge Research Systems) to give 14 bits of grayscale resolution. The vertical frame rate was 120 Hz and the mean luminance was about 45.3 cd/m^2.

Stimuli were presented in white mode at the center of the monitor screen in a square of 20 cm per side and were viewed at a distance of 143 cm subtending an area of 8° × 8°. The remainder of the screen was at mean luminance. The display spatial resolution was 64 pixels per degree of visual angle.

Stimulus presentation was programmed using Psychophysics Toolbox extensions to Matlab (Brainard, 1997; Pelli, 1997).

Stimuli construction

Digital images with 512 × 512 pixels with 8-bit range were constructed using Matlab. In Experiments 1 and 2, anisotropic noise stimuli were used (see examples in Figures 1a and 1d). In Experiment 1, the spatial window of the stimuli was Gaussian, and in Experiment 2, it was an annulus.

In Experiment 1, the stimulus was a complex moving noise with a spatial Gaussian window described by the following equation:

$$L(x,y,t) = L_0\left\{\begin{array}{l} 1 + m(t)\exp\left(-\dfrac{x^2+y^2}{2\sigma_{xy}^2}\right) \\ \\ \times\left[\begin{array}{l} m_1(t)\times n_1(x-v_1t,y) \\ +\, m_2(t)\times n_2(x-v_2t,y)\end{array}\right]\end{array}\right\}, \quad (1)$$

where n_1 and n_2 are anisotropic filtered white Gaussian noises with peak spatial frequencies of 1 and 3 cycles/deg, respectively (see the filter used in Equation 3); L_0 is the mean luminance, in cd/m^2; σ_{xy} is the spatial standard deviation, in degrees of visual angle (deg); m is the Michelson contrast as a function of time given by the next Gaussian function: $m(t) = \exp\{-t^2/(2\sigma_t^2)\}$, where σ_t is the temporal standard deviation, in milliseconds (ms); v_1 and v_2 are the velocities of each noise, in deg/s; m_1 and m_2 are the contrasts that were calculated to ensure that the two filtered noise samples have equal contrast energy.

In Experiment 2, the equation used to construct a complex moving noise with annulus window is

$$L(x,y,t) = L_0\left\{\begin{array}{l} 1 + m(t)\exp\left(-\left[\left(\sqrt{x^2\times y^2}\right) - r_i\right]^2 \Big/ 2\sigma_{xy}^2\right) \\ \\ \times\left[\begin{array}{l} m_1(t)\times n_1(x-v_1t,y) \\ +\, m_2(t)\times n_2(x-v_2t,y)\end{array}\right]\end{array}\right\}, \quad (2)$$

where r_i is the radius of the annulus, in degrees; the remaining symbols have the same meaning as in Equation 1.

To construct the anisotropic noise, first we generated a two-dimensional Gaussian white noise and then this noise was filtered using the following anisotropic Gaussian filter (Fourier transform of a 2D Gabor function):

$$|H(u,v)| = \left[\exp\left\{-2\pi^2\sigma_u^2(u-\rho_0)^2\right\} + \exp\left\{-2\pi^2\sigma_u^2(u+\rho_0)^2\right\}\right] \times \exp\{-2\pi^2\sigma_v^2v^2\}, \quad (3)$$

where the spreads of the Gaussian filter σ_u (parameter that determines the bandwidth in frequency) and σ_v (parameter that determines the bandwidth in orientation) were obtained by the following equations:

$$\sigma_u = \frac{\sqrt{\log(2)}(1+2^B)}{\rho_0\sqrt{2}\pi(2^B-1)}, \quad (4)$$

$$\sigma_v = \frac{\sqrt{\log(2)}}{\rho_0\sqrt{2}\pi\tan(\alpha/2)}, \quad (5)$$

where B = 1 octave (bandwidth in frequency, full width at half-height); α = 30 deg (bandwidth in orientation, full width at half-height); and the center frequency ρ_0 of the filter was 1 cycle/deg for the low spatial frequency noise (coarse scale) and 3 cycles/deg for the high spatial frequency noise (fine scale; see an example of the spectrum in Figures 1b, 1c, 1e, and 1f).

To equate both filtered noise samples (low and high) in energy, we need to calculate the contrasts m_1 and m_2. To obtain the values m_1 and m_2, we need to know the Root Mean Square contrast (c_{RMS}). For Experiments 1 and 2, it was 0.0748 for each filtered noise (see procedure to obtain the m value for a specific c_{RMS} in Serrano-Pedraza et al., 2007, their Equations 5, 6, and 7).

To construct moving noise, we created movies of 60 samples (one per frame), each frame was presented sequentially at a frame rate of 120 Hz. A different stochastic noise sample was used in each trial.

Procedure

Each trial started with a fixation cross displayed at the center of the screen using a Gaussian temporal function with standard deviation of 80 ms truncated to give an overall duration of 500 ms. Moving components always had a fixed speed of 4 deg/s. The motion direction, left or right, was randomized and the observer's task was to indicate, by pressing a mouse button, the direction they saw on each presentation. A new trial was initiated only after the observer's response, thus the experiment proceeded at a pace determined by the observer. For each stimulus and duration, 25 presentations were required. No feedback about the correctness of responses was provided.

In Experiments 1 and 2, five different configurations for the stimuli were used, three complex stimuli: stationary 1 cycle/deg noise with moving 3 cycles/deg noise; moving 1 cycle/deg noise with moving 3 cycles/deg noise both with the same direction of motion; moving 1 cycle/deg noise with stationary 3 cycles/deg noise; and two simple stimuli: moving 1 cycle/deg noise; and moving 3 cycles/deg noise. The stimuli were displayed using a temporal Gaussian function with a temporal standard deviation of $\sigma_t \in \{12.5, 25, 50\}$ ms (durations of $2\sigma_t \in \{25, 50, 100\}$ ms). The temporal Gaussian window was truncated to obtain the overall duration of 500 ms. Each experiment was carried out in different sessions. Once the fixation cross had disappeared the subjects saw one random presentation of the five possible configurations described above.

In Experiment 1 (Gaussian window), we used four sizes for the Gaussian window $\sigma_{xy} \in \{0.35, 0.7, 1.4, 2.8\}$ deg; and in Experiment 2 (annular window) , we used three radii $r_i \in \{1, 2, 3\}$ deg with a fixed size of the annulus of σ_{xy} = 0.35 deg.

In Experiment 3, complex Gabor patches were used because we needed a fine control of the contrast of the stimuli. The stimuli were constructed by adding a vertical moving Gabor patch of high spatial frequency (3 cycles/deg) to a static Gabor patch of low spatial frequency (1 cycle/deg). We used two sizes for the Gaussian window $\sigma_{xy} \in \{0.35, 1.4\}$ deg; three contrast for the static low frequency component $m_1 \in \{0.06, 0.12, 0.24\}$; and six contrast ratios between the contrast of the high frequency component (m_3) and the contrast of the low frequency component (m_1), $m_3/m_1 \in \{0.1, 0.2, 0.4, 0.8, 1, 1.6, 3.2, 6.4\}$. The stimuli were displayed using a temporal Gaussian function with a temporal standard deviation of σ_t = 12.5 ms (duration of $2\sigma_t$ = 25 ms).

Results

Experiment 1: Effect of stimulus size

The impaired motion perception of briefly presented moving stimuli containing both coarse-scale and fine-scale features occurs only with large stimuli. Neither the reversed perception, which occurs when moving fine features are combined with static coarse features, and the relatively poor performance, which occurs when coarse and fine features move together, occur with the smallest stimuli.

Figure 2b shows motion direction discrimination as a function of duration for simple and complex stimuli presented within Gaussian windows of different size. Each column shows results for stimuli of a different size (i.e., area) of the spatial Gaussian window ($\sigma_{xy} \in \{0.35, 0.7, 1.4, 2.8\}$ deg). For every stimulus, and for every size, performance is effectively perfect at the longest durations: plots converge in the upper right-hand corner of each panel.

Performance with the simple stimuli, in which the moving stimuli contain features of only a single scale (solid symbols), shows two trends. First, as noted above, discrimination improves with increasing duration and it is perfect at 100 ms. Second, there is a clear tendency, which can only be seen at short durations, for performance to decrease with increasing stimulus size. Performance is close

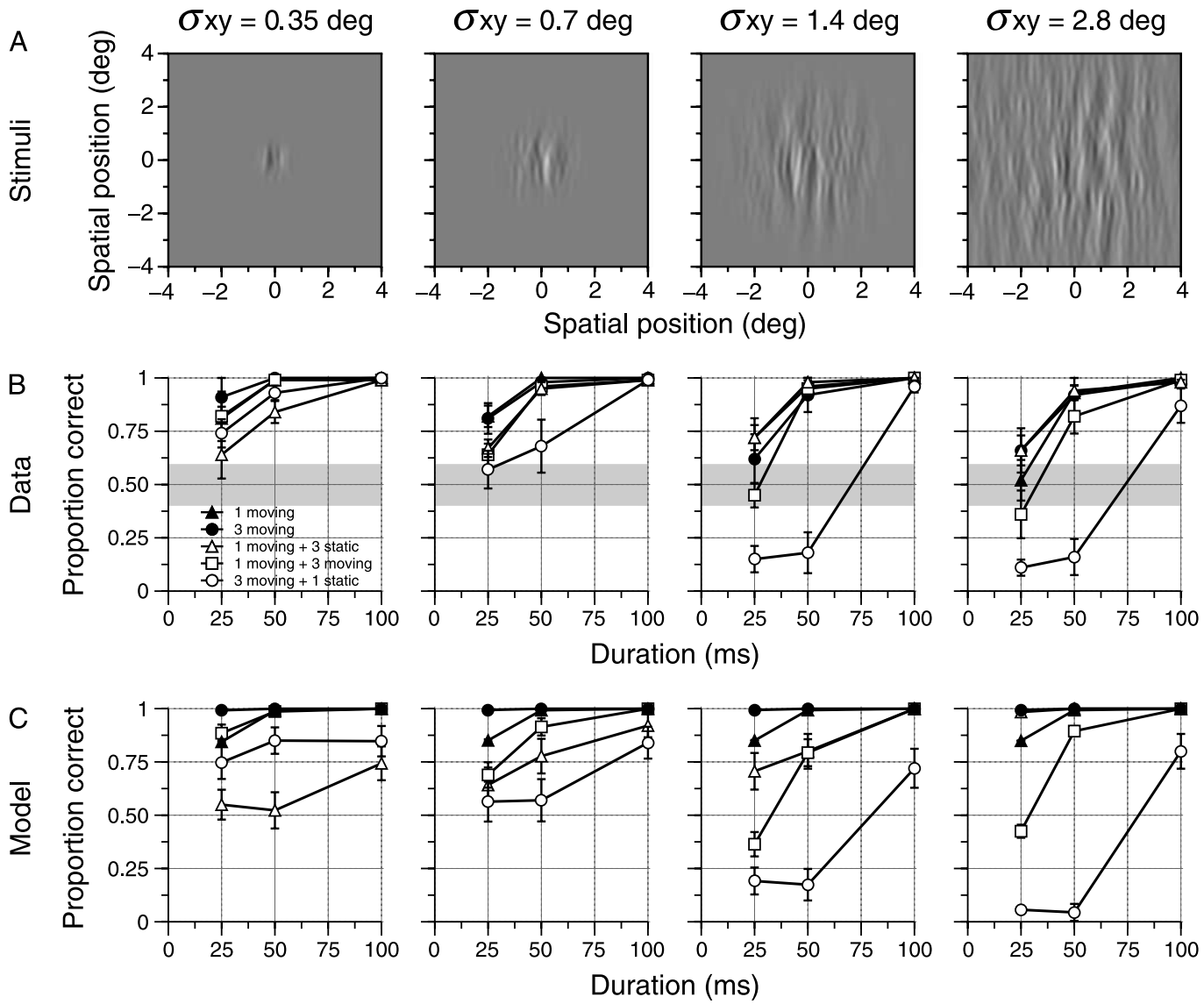

Figure 2. Results and model simulations of Experiment 1. (a) Examples of complex stimuli used in the experiment. The images are the sum of two octave-wide bands of noise centered on 1 and 3 cycles/deg with different Gaussian window sizes. (b) Means of the results ± *SEM* of four observers. Each column shows the results for different Gaussian window sizes. Each panel shows the horizontal direction-discrimination performance as a function of the duration of the temporal Gaussian window (duration = $2\sigma_t$). Open circles, stationary 1 cycle/deg noise with moving 3 cycles/deg noise; open squares, moving 1 cycle/deg noise with moving 3 cycles/deg noise; open triangles, moving 1 cycle/deg noise with stationary 3 cycles/deg noise; solid triangles, moving 1 cycle/deg noise; solid circles, moving 3 cycles/deg noise. Moving components had a fixed speed of 4 deg/s. The shaded area marks the 95% confidence limits assuming binomial variability for p = 0.5 and n = 100 using the score confidence interval (Wilson, 1927; see also Agresti & Coull, 1998). (c) Model predictions of Experiment 1 calculated using the same samples of anisotropic noise as were used in the experiment. Points are means of the proportion of correct responses obtained from 25 simulations of the model ± *SEM*.

to perfect for small Gaussian windows (σ_{xy} = 0.35 deg) and is close to chance for bigger Gaussian windows.

This kind of decline in motion-discrimination performance with increasing stimulus size has been observed before: Tadin, Lappin, Gilroy, & Blake (2003) found that, at high contrasts, increasing the size of a moving pattern renders its direction of motion more difficult to perceive. When both sets of noise are moving together (open squares), the same two trends are present: performance improves with increasing duration, and at short durations, performance declines with increasing stimulus size.

When the high spatial frequency noise is static (open triangles), the decline in performance at short durations and large window sizes is similar to that observed when it is absent. When the high frequency noise is moving, the decline is much more dramatic, and when the low spatial

frequency noise is static (open circles), performance is below 50% at the largest two window sizes. This decline below 50% indicates that the perceived direction of motion is reversed: performance is better than chance, but the perceived direction of motion is opposite to the true direction of motion. We have shown that the reversed percept can be modeled by incorporating a subtractive interaction between motion sensors tuned to high and low spatial frequencies (Serrano-Pedraza et al., 2007).

The fact that the reversals do not occur when the window is reduced in size suggests that the antagonism between motion sensors is not effective when the window size is smaller. We shall address the reason for this loss of reversals presently, but first we wish to explore the importance of two correlates of window size. First, we consider the fact that larger windows stimulate more peripheral retina, and so we repeat the experiment using annular windows of different radii.

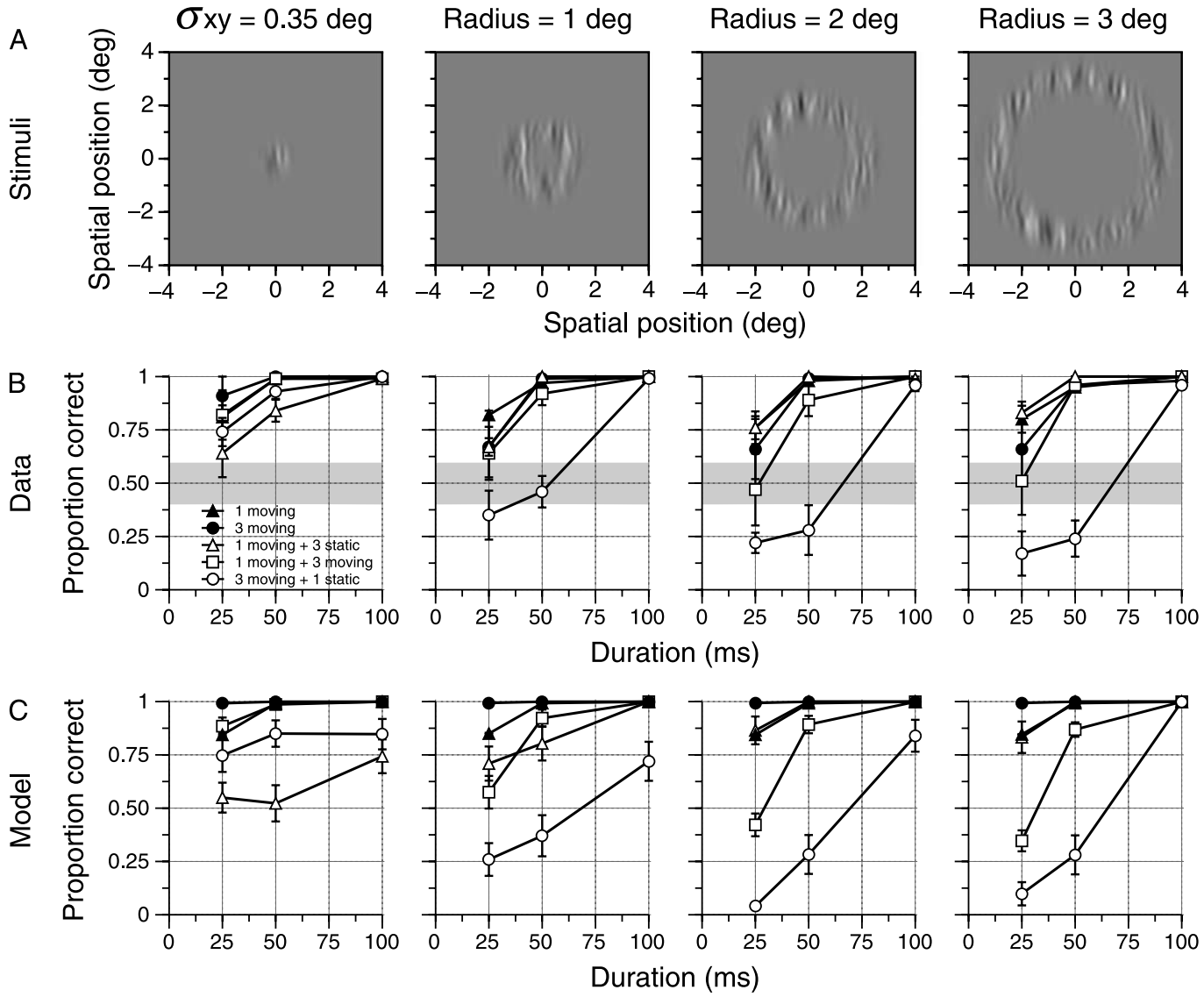

Figure 3. Results and model simulations of Experiment 2. (a) Examples of complex stimuli used in the experiment. The images are the sum of two octave-wide bands of noise centered on 1 and 3 cycles/deg with different radii of the annular window. (b) Means of the results ± *SEM* of four observers. The first column shows the same results shown in the first column of Figure 2. The other three columns show the results for different annular windows. Each panel shows the horizontal direction-discrimination performance as a function of the duration of the temporal Gaussian window (duration = $2\sigma_t$). Open circles, stationary 1 cycle/deg noise with moving 3 cycles/deg noise; open squares, moving 1 cycle/deg noise with moving 3 cycles/deg noise; open triangles, moving 1 cycle/deg noise with stationary 3 cycles/deg noise; solid triangles, moving 1 cycle/deg noise; solid circles, moving 3 cycles/deg noise. Moving components had a fixed speed of 4 deg/s. The shaded area marks the 95% confidence limits assuming binomial variability for $p = 0.5$ and $n = 100$ using the score confidence interval. (c) Model predictions of Experiment 2 calculated using the same samples of anisotropic noise as were used in the experiment. Points are means of the proportion of correct responses obtained from 25 simulations of the model ± *SEM*.

Experiment 2: Effect of near periphery

Figure 2 shows very clearly that the reversals in the perception of the direction of motion of complex stimuli do not occur with small stimuli. However, the large stimuli differ from the small stimuli in the extent that they fall on peripheral retina. In order to test whether stimuli that fall on peripheral retina but do not stimulate the fovea also cause reversals, we repeated the experiment using annular windows.

Figure 3b shows motion direction discrimination as a function of duration for simple and complex stimuli presented inside annular windows of different radii. As in Figure 2, each row shows the performance discriminating the direction of motion of five different combinations of fine-scale (3 cycles/deg) and coarse-scale (1 cycle/deg) noises, plotted against the duration for which the stimulus was presented. Each column shows results for stimuli of a different radius of the annular window ($r_i \in \{1, 2, 3\}$ deg). The leftmost panel shows the same results as in the leftmost panel of Figure 2b (σ_{xy} = 0.35 deg) just for comparison.

The results are very similar to those shown in Figure 2b despite the differences in the spatial window shape. The reversals in motion discrimination that occur when high frequency noise moves and low frequency noise is static (open circles) are present in all four subjects for the largest two annular windows and diminish as the radius is reduced.

These results suggest that reversals that occur when the window is large depend primarily on the periphery because a very similar pattern of reversals occurs with annular windows, which do not stimulate the fovea. However, we cannot discount the importance of stimulus area because the area of an annular window increases with its radius.

Experiment 3: Effect of relative contrast

We know that the reversals in perceived motion of complex stimuli can be modeled by antagonism between coarse and fine motion sensors (Serrano-Pedraza et al., 2007). We would expect the perceptual effect of this antagonism to depend on the balance in activity between coarse and fine motion sensors. In Experiment 3, we tested this idea by changing the relative contrast of the components of a complex stimulus in order to affect the balance between coarse and fine sensors. In order to allow a greater range of contrasts, we used Gaussian-windowed 1 cycle/deg and 3 cycles/deg gratings, Gabor patches, instead of patches of filtered noise.

We used two different sizes of Gaussian window, one small (σ_{xy} = 0.35 deg) and one bigger (σ_{xy} = 1.4 deg), and

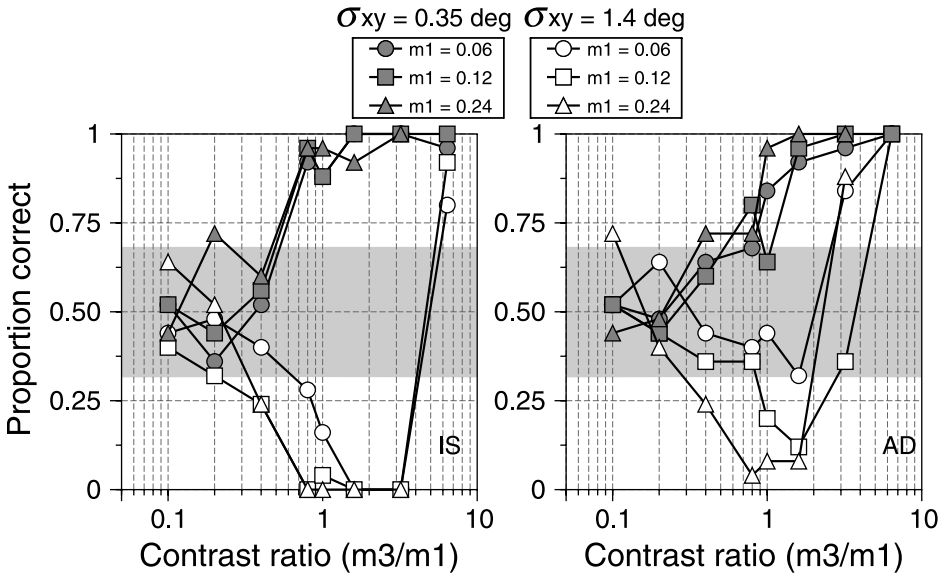

Figure 4. Results from Experiment 3 for two subjects (IS and AD). In this experiment, the complex stimuli were constructed by adding a vertical moving Gabor patch of high spatial frequency (3 cycles/deg) to a static Gabor patch of low spatial frequency (1 cycle/deg). Panels show the horizontal direction-discrimination performance of the moving high frequency component as a function of the ratio between its contrast (m3) and the contrast (m1) of the low frequency component. Each panel shows the results for one observer. Dark symbols represents the results for the complex stimuli windowed by a Gaussian window of σ_{xy} = 0.35 degrees; white symbols, results for a Gaussian window of σ_{xy} = 1.4 degrees. The different shapes show the results obtained with different contrasts of the stationary 1 cycle/deg Gabor patch, m1. Circles, m1 = 0.06; squares, m1 = 0.12; and triangles, m1 = 0.24. The moving component of high frequency had a fixed speed of 4 deg/s. The duration of the temporal Gaussian window was 25 ms for all conditions. There were 25 observations per point. Other details as for Figure 2.

changed the absolute and the relative contrast of the components of the complex stimulus in order to affect the balance between the mechanisms. We expect that for both windows, the reversals will appear for a limited range of contrasts as previously shown for big windows by Derrington and Henning (1987).

Figure 4 shows that the reversals do not occur with small stimuli, and that with large stimuli they appear to depend more on absolute contrast than on relative contrast. The panels show the proportion of correct motion discrimination of moving 3 cycles/deg grating (speed of 4 deg/s) presented at short durations (25 ms) as a function of the contrast ratio between the moving 3 cycles/deg grating and the static 1 cycle/deg grating.

Reversals only occur with the larger stimulus (σ_{xy} = 1.4 deg, white symbols). When the contrast of the low frequency component is high, there is a slight tendency for reversals, indicated by performance below 0.5, to occur for a wider range of relative contrasts. However, in all cases, at the highest contrast ratios, performance rises above 0.5, indicating that motion is seen in the correct direction. This pattern of performance presumably reflects the fact that the high-contrast, brief, low spatial-frequency component of the stimulus activates motion sensors tuned to opposite directions of motion. It activates both directions equally because it is static. When the moving high spatial frequency component is introduced, its motion is not as salient as the reversed motion percept caused by the fact that it disturbs the balance between the low spatial frequency motion sensors. Consequently, the dominant sensation is one of reversed motion. When its contrast is high, the high spatial frequency stimulus gives rise to a more salient sense of motion in the correct direction.

With the smaller window size (σ_{xy} = 0.35 deg, dark symbols), no reversals were found and the proportion of correct responses increases with the contrast ratio from chance to perfect performance. The lack of reversals when the window size is small could be caused by the fact that low spatial frequency motion sensors are not strongly activated by a small stimulus.

Model simulations

We used a simple model (see Serrano-Pedraza et al., 2007, their Appendix A) to test our proposal that the impaired motion discrimination and the reversals in perceived direction we describe here reflect inhibitory interactions between motion sensors tuned to high spatial frequencies and those tuned to low spatial frequencies. The only modification that we have made in the model with respect to Serrano-Pedraza et al. (2007) is that we increased the number of sensor locations in order to cover a larger area because in this paper we used bigger spatial windows.

The basic motion analyzer is a hybrid of two well-established models (Adelson & Bergen, 1985; Watson & Ahumada, 1985). It uses the computational approach of Adelson and Bergen's motion energy detector but takes some of the filter parameters from Watson and Ahumada's linear motion sensor. To compute the model responses, the basic sensor is replicated at 6 orientations (−60°, −30°, 0°, 30°, 60°, 90°) and 2 spatial frequencies (1 and 3 c/deg) at 49 locations covering an 8° × 8° patch. The locations of the sensors were $x' \in \{-3, -2, -1, 0, 1, 2, 3\}$ deg and $y' \in \{-3, -2, -1, 0, 1, 2, 3\}$ deg. The equations and parameters of the spatial weighting functions of the sensors and the temporal impulse response functions are the same as described in Serrano-Pedraza et al. (2007); their Appendix, Equations A1 and A6). Sensor responses to movies used in experiments are calculated (by the inner product of the stimulus with the spatial weighting function of the sensor and convolving the output with the temporal impulse response) within each orientation band and summed across locations. The high frequency response is subtracted from the low frequency response (and vice versa) for the same direction of motion (right or left) and orientation. Responses are half-wave rectified and pooled across different orientations using cosine weighting and the final response is taken from the spatial frequency channel that has the highest difference between right and left. The highest difference is converted to a direction index and then converted into a performance score using a sigmoidal response function in order to obtain the probability of correct response. It is important to notice that the model is not fitted to the psychophysical data; the parameters of the model were fixed a priori and were always the same for all simulations.

Although the model implements summation between the sensors of the same tuned spatial frequency, it has obvious limitations. For example, the model does not implement either complex spatial interactions like surround suppression (Tadin et al., 2003) or anisotropic surround suppression (Rajimehr, 2005) Therefore, we can anticipate that the model will not explain either the reduction in direction-discrimination performance that occurs when a single frequency stimulus increases in size or the differences in direction discrimination given by anisotropic characteristics of the spatial windows of the stimulus.

Simulation results

Figures 2c and 3c show the results generated from the calculated responses of the model to the stimuli used in Experiments 1 and 2, respectively. The model responses show the same basic features as the psychophysical results in Figures 2b and 3b.

Figure 2c shows that the model's estimate of the direction of motion of high spatial frequency orientation-filtered noise reverses at short durations when the noise is presented with static low spatial frequency noise with spatial Gaussian windows bigger than 1.4 degrees. It also shows that the reversals in direction disappear if the stimulus is reduced in size from 2.8 deg to 0.35 deg radius.

Figure 3c shows that similar reversals occur with annular windows. It also shows that if the stimulus is presented within an annular window with small radius (1 deg), errors almost disappear, but they return if the radius is made bigger than 2 deg.

Figure 5 shows the simulation results of Experiment 3. We used the same two sizes of the complex stimulus and the three Michelson contrasts used in the experiment for the low frequency component. We performed the simulations using the same number of contrast ratios. We also implemented a direction-discrimination threshold so that, if the energy of the moving stimulus was lower than the energy of a 3 cycles/deg Gabor patch of 5% contrast presented with a duration of 25 ms with a window size of σ_{xy} = 0.35 degrees, then the probability of correct response was 0.5. This threshold only makes a difference to the response of the model when the window is small and the contrast ratio is low. It is probable that the addition of noise either to the stimulus or to the responses of the motion sensors would remove the need for a threshold but that is beyond the scope of this paper.

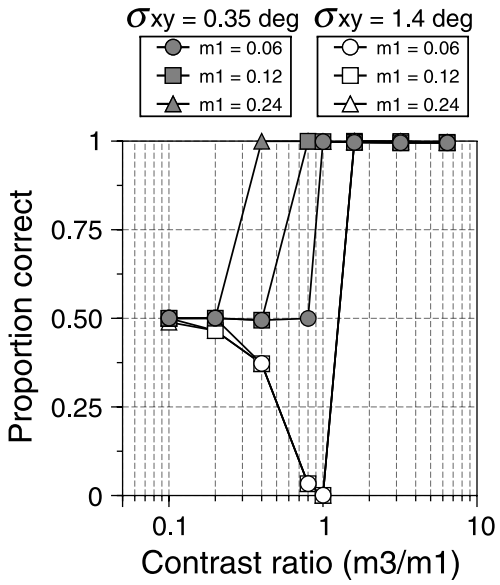

Figure 5. Model simulations of Experiment 3. Points represent the proportion of correct responses as a function of the contrast ratio between the contrast of the high frequency component (m3) and the contrast of the low frequency component (m1). Dark symbols represents the results for the complex stimuli windowed by a Gaussian window of σ_{xy} = 0.35 degrees; white symbols, results for a Gaussian window of σ_{xy} = 1.4 degrees. The different shapes show the simulations performed with different contrasts of the stationary 1 cycle/deg Gabor patch; circles, m1 = 0.06; squares, m1 = 0.12; and triangles, m1 = 0.24.The moving component of high frequency had a fixed speed of 4 deg/s. The duration of the temporal Gaussian window was 25 ms for all conditions.

The results of the simulation were similar to those obtained in Experiment 3. For the largest simulated size (σ_{xy} = 1.4 degrees, white symbols), independently of the contrast of the low frequency component, the proportion of correct responses is at chance for contrast ratios from 0.1 to 0.4, then reversals in direction discrimination appear for ratios from 0.8 to 1, and finally the proportion of correct responses goes to perfect performance for higher contrast ratios. However, the results show that for the smallest size tested (σ_{xy} = 0.35 degrees, dark symbols), independently of the contrast of the low frequency component, no reversals were found and the proportion of correct responses increased with the contrast ratio from chance to perfect performance.

Discussion

The results show that when a brief moving stimulus contains both fine and coarse features, motion of the fine features when the coarse features are static causes failures (or reversals) in the perceived direction of motion. The same kind of failures have been reported previously (Derrington et al., 1993, Derrington & Henning, 1987, Henning & Derrington, 1988; Serrano-Pedraza et al., 2007).

The novel aspect of the results reported here is that Experiments 1 and 2 show that the perceptual failures depend on the size of the stimulus, both for Gaussian- and annular-windowed stimuli. The reversals in perceived direction of motion disappear if the Gaussian-windowed stimulus has a standard deviation of 0.7 deg or less, and if the annular-windowed stimulus has a radius of 1 deg or less.

Another novel result is shown by Experiment 3. The reversals in motion direction discrimination disappear for very small window size (0.35 deg), regardless of the contrast ratio between moving fine-scale and static coarse-scale features. In this experiment, we have also shown that when the size of the stimulus is 1.4 degrees the reversals in direction discrimination appeared only within a small range of contrast ratios replicating in this way the results reported by Derrington and Henning (1987).

The model demonstrates that simple subtractive interactions between motion sensors tuned to the same direction but different spatial frequencies can account for the variation in reversals with stimulus size and contrast.

This hypothetical antagonism between motion sensors sensitive to different spatial frequencies but the same direction of motion could contribute to the explanation of a number of phenomena reported in recent literature. The

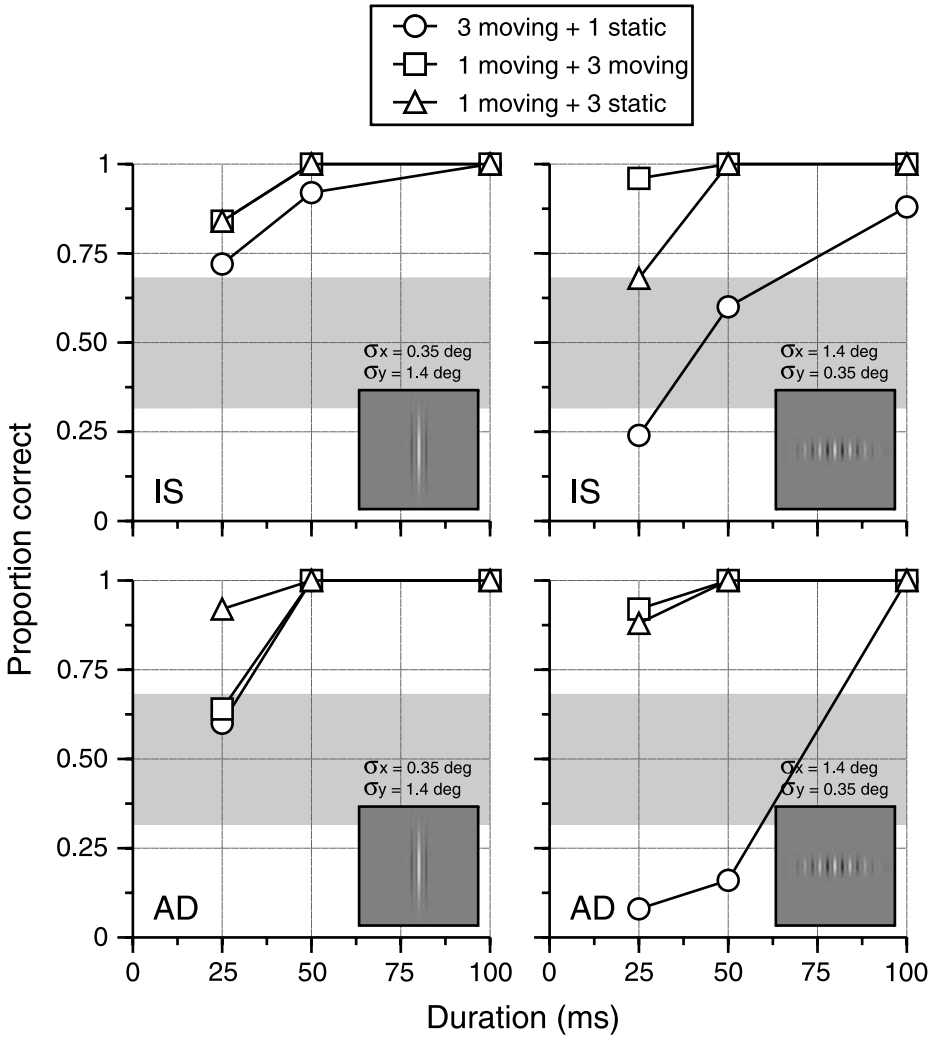

Figure 6. Results from the control experiment for two subjects (IS and AD). Top row shows the results for subject IS and bottom row for subject AD. Left panels show the results for spatial Gaussian windows with spatial deviations of σ_x = 0.35 degrees and σ_y = 1.4 degrees; right panels, results for σ_x = 1.4 degrees and σ_y = 0.35 degrees. Each panel shows the horizontal direction-discrimination performance as a function of the duration of the temporal Gaussian window (duration = $2\sigma_t$). In each panel, there is an example of the stimulus used in each experimental condition. Open circles, stationary 1 cycle/deg Gabor patch with moving 3 cycles/deg Gabor patch; open squares, moving 1 cycle/deg Gabor patch with moving 3 cycles/deg Gabor patch; open triangles, moving 1 cycle/deg Gabor patch with stationary 3 cycles/deg Gabor patch. The moving components had a fixed speed of 4 deg/s. There were 25 observations per point per subject. Other details as for Figure 2.

antagonism could help explain reversals in perceived direction of motion of second-order modulations (Cropper, Kvansakul, & Johnston, 2009) and the asymmetric shape of the motion after-effect tuning functions (Ledgeway & Hutchinson, 2009) and could also help explain why subjects judge motion direction based on motion signals from low spatial frequencies rather than high spatial frequencies (Hayashi, Sugita, Nishida, & Kawano, 2010).

Reversals in perceived motion occur when two conditions are fulfilled.

1. First, the coarse sensors for opposite directions of motion must *both* have a strong signal. This will occur when the stimulus is a briefly presented static (or slowly moving) low spatial frequency pattern, which is sufficiently large in size and high in contrast.
2. Second, there must be a moderately strong signal for one direction only in the high spatial frequency sensors.

When both conditions occur, the signal in the high frequency sensors disturbs the balance between the opposed signals in the low frequency sensors and reversed motion is seen.

If the signal in the high spatial frequency motion sensors is too strong, as occurs at the highest contrasts in

Experiment 3, then the high frequency sensors dominate perception and motion is seen in the correct direction.

The errors disappear when stimulus size is reduced. A reduction in stimulus size reduces differentially the response of the low spatial frequency motion sensors so that condition 1 no longer applies. According to the model used here, the differential reduction of the response of the low spatial frequency sensors can be explained by the different spatial characteristics and the relative sensor gains of the motion sensors. For example, both high and low frequency sensors (Gabor functions) have a bandwidth of 1 octave in spatial frequency (σ_x) and 30 degrees in orientation (σ_y). These values are relative to the spatial frequency of the sensor so for the low frequency sensors the dimensions of the spatial window are $\sigma_x = 0.5622$ and $\sigma_y = 0.6994$; and for the high frequency sensors, the dimensions are smaller: $\sigma_x = 0.1874$ and $\sigma_y = 0.2331$. Because the small stimulus ($\sigma_{xy} = 0.35$) is smaller than the receptive field of the low frequency sensors, the response of those sensors is reduced considerably. However, even the small stimulus is larger than the receptive field dimensions of the high frequency sensors so there is no significant reduction in response. Consequently, when the stimulus size is reduced, condition 1 above fails to apply. The response of the high frequency sensors dominates perception because the response of the low frequency sensors is too small for any imbalance to give rise to a motion percept and therefore motion will be seen in the correct direction.

Experiment 1 with 2D Gaussian windows and Experiment 2 with annular windows show similar effects of window size. This raises the possibility that the linear extent of the stimulus window may be more important than its area. We carried out a small control experiment to test this possibility and to test the relative importance of horizontal extent (i.e., extent in a direction orthogonal to the grating stripes, parallel to the axis of motion) and vertical extent (in a direction parallel to the grating bars, orthogonal to the axis of motion).

We measured the discrimination of motion direction as a function of duration for complex stimuli (Gabor patches) presented within two different oval Gaussian windows (see details in Figure 6). The results show that reversals occur when the oval window is horizontally elongated along the axis of motion (Figure 6, right panels). However, when the oval window is vertically elongated (Figure 6, left panels) the reversals disappear. This experiment is very interesting because it shows that in order to produce reversals the elongation of the window along the axis of motion is more important than the elongation orthogonal to the axis of motion and suggests that the region of support of the inhibitory motion mechanisms may be elongated along the axis of motion. A similar elongation has been observed in the receptive fields of motion-selective neurons selective for low spatial frequencies in marmoset V1 (Tinsley et al., 2003).

It is important to note that the model as it is did not reproduce these results obtained with oval windows. This opens a door to future modifications of the model, in which this anisotropy should be implemented.

Acknowledgments

Some of the findings described have been reported previously in the European Conference on Visual Perception 2008 (Serrano-Pedraza & Derrington, 2008). We thank Sophie Wuerger and Jenny C. A. Read for helpful comments on the manuscript.

Commercial relationships: none.
Corresponding author: Ignacio Serrano-Pedraza.
Email: i.s.pedraza@ncl.ac.uk.
Address: Henry Wellcome Building, Framlington Place, Newcastle upon Tyne, NE2 4HH, UK.

References

Adelson, E. H., & Bergen, J. R. (1985). Spatiotemporal energy models for the perception of motion. *Journal of the Optical Society of America A, Optics, Image Science, and Vision, 2,* 284–299. [PubMed]

Agresti, A., & Coull, B. (1998). Approximate is better than "exact" for interval estimation of binomial proportions. *American Statistician, 52,* 119–126.

Anderson, S. J., & Burr, D. C. (1985). Spatial and temporal selectivity of the human motion detection system. *Vision Research, 25,* 1147–1154. [PubMed]

Anderson, S. J., & Burr, D. C. (1987). Receptive field size of human motion detection units. *Vision Research, 27,* 621–635. [PubMed]

Anderson, S. J., & Burr, D. C. (1989). Receptive field properties of human motion detector units inferred from spatial frequency masking. *Vision Research, 29,* 1343–1358. [PubMed]

Anderson, S. J., & Burr, D. C. (1991). Spatial summation properties of directionally selective mechanisms in human vision. *Journal of the Optical Society of America A, 8,* 1330–1339. [PubMed]

Anderson, S. J., Burr, D. C., & Morrone, M. C. (1991). Two-dimensional spatial and spatial-frequency selectivity of motion-sensitive mechanisms in human vision. *Journal of the Optical Society of America A, 8,* 1340–1351. [PubMed]

Brainard, D. H. (1997). The psychophysics toolbox. *Spatial Vision, 10,* 433–436. [PubMed]

Cropper, S. J., Kvansakul, J. G. S., & Johnston, A. (2009). The detection of the motion of contrast modulation: A

parametric study. *Attention, Perception, & Psychophysics, 71,* 757–782. [PubMed]

Derrington, A. M., Fine, I., & Henning, G. B. (1993). Errors in direction-of-motion discrimination with dichoptically viewed stimuli. *Vision Research, 33,* 1491–1494. [PubMed]

Derrington, A. M., & Henning, G. B. (1987). Errors in direction-of-motion discrimination with complex stimuli. *Vision Research, 27,* 61–75. [PubMed]

Hayashi, R., Sugita, Y., Nishida, S., & Kawano, K. (2010). How motion signals are integrated across frequencies: Study on motion perception and ocular following responses using multiple-slit stimuli. *Journal of Neurophysiology, 103,* 230–243. [PubMed]

Henning, G. B., & Derrington, A. M. (1988). Direction-of-motion discrimination with complex patterns—Further observations. *Journal of the Optical Society of America A, Optics, Image Science, and Vision, 5,* 1759–1766.

Ledgeway, T., & Hutchinson, C. V. (2009). Visual adaptation reveals asymmetric spatial frequency tuning for motion. *Journal of Vision, 9*(1):4, 1–9, http://www.journalofvision.org/content/9/1/4, doi:10.1167/9.1.4. [PubMed] [Article]

Pelli, D. G. (1997). The VideoToolbox software for visual psychophysics: Transforming numbers into movies. *Spatial Vision, 10,* 437–442. [PubMed]

Rajimehr, R. (2005). Anisotropic center–surround antagonism in visual motion perception [Abstract]. *Journal of Vision, 5*(8):133, 133a, http://www.journalofvision.org/content/5/8/133, doi:10.1167/5.8.133.

Serrano-Pedraza, I., & Derrington, A. M. (2008). Errors in direction of motion at short durations depend on stimulus size and eccentricity. *Perception, 37,* 26–27.

Serrano-Pedraza, I., Goddard, P., & Derrington, A. M. (2007). Evidence for reciprocal antagonism between motion sensors tuned to coarse and fine features. *Journal of Vision, 7*(12):8, 1–14, http://www.journalofvision.org/content/7/12/8, doi:10.1167/7.12.8. [PubMed] [Article]

Tadin, D., Lappin, J. S., Gilroy, L. A., & Blake, R. (2003). Perceptual consequences of centre–surround antagonism in visual motion processing. *Nature, 424,* 312–315. [PubMed]

Tinsley, C., Webb, B., Barraclough, N., Vincent, C., Parker, A., & Derrington, A. M. (2003). The nature of V1 neural responses to 2D moving patterns depends on receptive-field structure in the Marmoset monkey. *Journal of Neurophysiology, 90,* 930–937. [PubMed]

Watson, A. B., & Ahumada, A. J. J. (1985). Model of human visual-motion sensing. *Journal of the Optical Society of America A, 2,* 322–342. [PubMed]

Wilson, E. B. (1927). Probable inference, the law of succession, and statistical inference. *Journal of the Statistical Association, 22,* 209–212.